
Feasibility of medical radioisotope production based on the proton beams at China Spallation Neutron Source

Bing Jiang ^{1,2}, Binbin Tian ^{1,2}, Hantao Jing ^{1,2,*}, Qifan Dong ^{1,2,3}

¹Spallation Neutron Source Science Center, Dongguan 523803, China

²Institute of High Energy Physics, Chinese Academy of Sciences (CAS), Beijing 100049, China

³University of Chinese Academy of Sciences, Beijing 100049, China

*Corresponding author. *E-mail address:* jinght@ihep.ac.cn

Abstract: The utilization of a proton beam from the China Spallation Neutron Source (CSNS) for producing medical radioisotopes is appealing owing to its high current intensity and high energy. The medical isotope production based on the proton beam at the CSNS is significant for the development of future radiopharmaceuticals, particularly for the α -emitting radiopharmaceuticals. The production yield and activity of typical medical isotopes were estimated using the FLUKA simulation. The results indicate that the 300-MeV proton beam with a power of 100 kW at CSNS-II is highly suitable for proof-of-principle studies of most medical radioisotopes. In particular, this proton beam offers tremendous advantages for the large-scale production of alpha radioisotopes, such as ^{225}Ac , whose theoretical production yield can reach approximately 57 Ci/week. Based on these results, we provide perspectives on the use of CSNS proton beams to produce radioisotopes for medical applications.

Key words: CSNS proton beam; Medical isotope production; α -emitting radionuclides; nuclidic purity analysis

1. Introduction

Nuclear medicine is a special radioisotope carrier that uses radiation to provide diagnostic information regarding the function of a person's specific organs or to treat them [1]. Since the discovery of the diagnostic and treatment abilities of nuclear medicine in the last century, a wide variety of medical radioisotopes have been studied and developed to enhance the treatment of cancer and other diseases. Currently, over 40 million nuclear medicine procedures are performed annually, and the demand for radioisotopes has increased by up to 5% [1]. For example, diagnostic radioisotopes such as technetium-99 ($^{99\text{m}}\text{Tc}$) and therapeutic radioisotopes like actinium-225 (^{225}Ac) are increasingly being utilized in the field of radiopharmaceuticals, with corresponding minimum activities for pharmaceutical purposes of 40 and 0.1 mCi, respectively. The production of

radioisotopes has gained significant prominence in the development of the national economy and healthcare because of their extensive applications in nuclear technology, particularly in nuclear medicine. In China, the *Medium- and Long-Term Development Plan for Medical Isotopes (2021–2035)* was officially issued by eight ministries and commissions in June 2021 to study the production and application of medical radioisotopes as a national strategy. Compared to the international need, the objective of this plan is to accomplish the key technological development of medical isotopes including ^{99}Mo , $^{68}\text{Ge}/^{68}\text{Ga}$, $^{123,124}\text{I}$, $^{64,67}\text{Cu}$, ^{89}Zr , ^{103}Pd , ^{111}In , and ^{225}Ac , as well as to master core competencies in irradiation structure design, optimization of irradiation parameters, post-processing of targets, and recovery of essential raw materials. This is of great significance for improving the capacity of radioisotope-related industries and ensuring the implementation of the Healthy China strategy, which covers public health services, environmental management, the Chinese medical industry, and food and drug safety^[2].

Radioisotopes can be generated through the irradiation of stable isotope targets in nuclear reactors or particle accelerators^{[3]–[9]}. As an effective supplement to isotope production using reactors, irradiation with an accelerator provides a new pathway for generating neutron-deficient nuclides and developing innovative medical radioisotopes. Using high-intensity proton or gamma-ray beam facilities, appropriate targets can be exposed to the particle irradiation and undergo proton- or photon-nuclear reaction to produce new radioisotopes such as $^{99\text{m}}\text{Tc}$ and ^{225}Ac ^{[9][10]}. More than 3000 low-energy medical cyclotrons are being used worldwide for the production of traditional medical radioisotopes, such as ^{18}F . However, only a few proton accelerators with energies greater than 100 MeV have been used for radioisotope production. To produce specific radioisotopes with high chemical purity according to pharmacopoeia limits, several dedicated facilities for radioisotope research have been constructed at high-energy particle accelerator centers globally. For example, in Switzerland, the 1.4-GeV CERN-MEDICIS (MEDical Isotopes Collected from ISolde) facility delivered its first radioactive ion beam at CERN in December 2017 to support the research and development of nuclear medicine using non-conventional radioisotopes, such as $^{149,152,155}\text{Tb}$, ^{153}Sm , $^{165,167}\text{Tm}$, ^{169}Er , ^{175}Yb , and ^{225}Ac ^[9]. In Canada, the Isotope Separator and Accelerator (ISAC) facility at TRIUMF is a powerful source for producing research quantities of promising therapeutic radioisotopes for feasibility studies^[11]. In China, a 100-MeV compact cyclotron, CYCIAE-100, has

been designed and constructed at CIAE (China Institute of Atomic Energy) to be used as a driver for the BRIF (Beijing Radioactive Ion-beam Facility)^{[12][13]}, which is highly suitable for the radioisotopes production due to its high beam current up to 520 μ A.

China Spallation Neutron Source (CSNS) is a proton-driven complex that provides multidisciplinary platforms for scientific research and applications^{[14]-[16]}. In CSNS phase I (CSNS-I), a tungsten coated tantalum (W-Ta) spallation target was bombarded with a 1.6 GeV proton beam with an accelerator power of 100 kW and a repetition rate of 25 Hz. Presently, an important upgrade of the facility, namely CSNS phase II (CSNS-II), which will increase the power of protons to 500 kW, is ongoing. In parallel, a design study for beam quality improvement and an upgrade in proton beam intensity and energy is also being performed. A 300-MeV proton beam can be extracted from the end of the H⁻ Linear accelerator at CSNS-II to carry out irradiation experiments. This beamline can provide a power of at least 100 kW for radioisotope production, providing a competitive advantage among similar international facilities. This study aimed to analyze the feasibility of medical radioisotope production using proton beams at the CSNS.

The remainder of this paper is organized as follows. Section 2 provides a detailed description of proton beams at the CSNS. Section 3 describes the simulation method and the irradiation of target materials for medical isotope production. The in-target production yields of typical medical isotopes are presented in Section 4. Finally, the conclusions are presented in Section 5.

2. Medium proton beams at CSNS

The CSNS facility consists of an H⁻ Linear accelerator (LINAC), a proton rapid cycling synchrotron (RCS), a target station, and several neutron experimental spectrometers^{[17]-[19]}. A proton beam with medium energy can be extracted from the end of the LINAC, which is suitable for applications in proton irradiation, particularly in medical radioisotope production. The basic parameters of the proton beamlines at the CSNS are summarized in **Table 1**, and the details are described in the following subsections.

Table 1. Basic parameters of the proton beams at CSNS.

| Beam line | Project | Extraction position | Maximum Energy (MeV) | Power (kW) | Intensity (μ A) |
|-----------|---------|---------------------|-------------------------|---------------|-------------------------|
| APEP | CSNS-I | LINAC | 80 | 0.016-5 | 0.2 - 62.5 |
| APEP | CSNS-II | LINAC | 300 | 100 | 333.3 |

Associated Proton Beam Experiment Platform (APEP) beamline is the first proton irradiation facility to utilize naturally stripped protons extracted from the H⁻ LINAC at the CSNS. The accelerated H⁻ ion beams interacted with the residual gas in the vacuum tube, among which a small number of the H⁻ ions were stripped into protons and transported to the end of the LINAC. The physical design of the APEP beamline, including the proton transport, beam collimation, and radiation shielding, can be found in [20].

Figure 1 shows the schematic drawing of the APEP beamline, whose actual length is approximately 14.5 m. Two experimental irradiation points, namely the vacuum test point (VTP) and the air test point (ATP), are located on the beamline at flight path lengths of approximately 9.3 and 10 m from the extraction position, respectively. A wedge degrader, which allows a continuous change in the thickness, was used to continuously adjust the proton energy within the range of 10–80 MeV. To satisfy different experimental requirements, a cascading collimation system consisting of three graphite collimators was employed to control the spot sizes, which resulted in beam spot sizes ranging from 10 mm × 10 mm to 50 mm × 50 mm at the irradiation points.

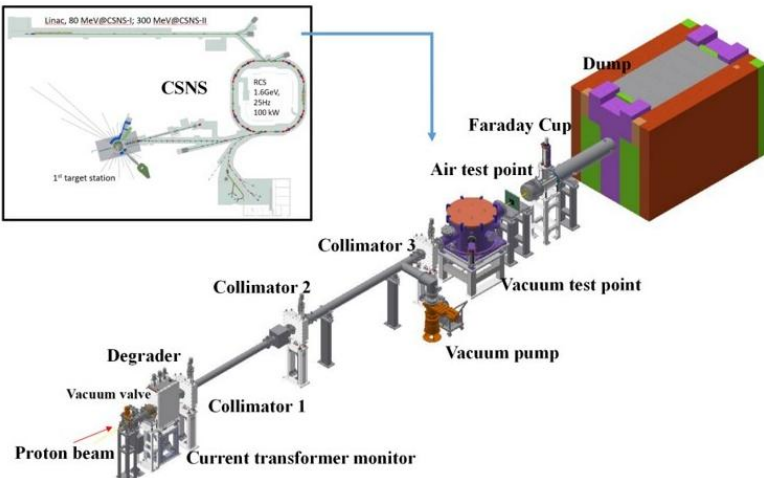


Fig.1. Layout of the APEP.

By utilizing a degrader to adjust the proton energy, a series of irradiation experiments on medical isotopes of interest, such as $^{123,125}\text{I}$, ^{103}Pd , $^{99\text{m}}\text{Tc}$, ^{82}Sr , ^{68}Ge , ^{64}Cu , and ^{62}Zn , can be performed at both the vacuum and air test points with a proper target material. These isotopes are extensively used in the medical field with a relatively high production cross-section at low proton energies, which is ideal for carrying out verification experiments under the present experimental conditions provided by the APEP.

Tables 2 and **3** list the medical isotopes with potential for APEP production and research. For the 80-MeV (CSNS-I) and 300-MeV (CSNS-II) APEP beamlines, the recommended medical isotopes and corresponding reaction channels are provided, as well as suitable medical applications. The medical isotopes produced by APEP are not limited to those listed in the tables. These isotopes are widely used in medical applications^{[1][11][13][21]}. In general, the 80-MeV APEP can meet the requirements of production experiments for most medical isotopes and the proof-of-principle of some innovative alpha isotopes (see **Table 2**). With the help of appropriate gamma spectroscopy, two types of experiments can be carried out at 80-MeV APEP at present: (1) quantitative analysis of the end of bombardment (EOB) activity in the irradiated targets; (2) proton-induced reaction cross-section measurement based on the activation analysis technique. The EOB activity of the specific isotope is deduced by using the characteristic γ -ray count of the decay products, while the proton-induced reaction cross section can be calculated by the EOB activity and the incident proton intensity. The latter is generally measured by placing appropriate monitoring targets in a proton beam that receives irradiation simultaneously with the experimental target. The CSNS-I APEP line started operation in 2021, and its application in user experiments has also begun. Recently, an irradiation experiment of ^{100}Mo target was performed at the APEP, and an experimental yield of a $^{99\text{m}}\text{Tc}$ conforming to the theoretical calculation was obtained. Based on APEP, a 2-h irradiation of a multi-layer ^{100}Mo target can produce approximately 60 MBq of $^{99\text{m}}\text{Tc}$ and 18 MBq of ^{99}Mo sufficient for pre-clinical studies. Further details can be found in^[22].

Table 2. Typical medical isotopes produced by proton beam with the energy up to 80 MeV (CSNS-I, APEP).

| Medical Isotope | Half-Life | Reaction Channel | Proton Energy(MeV) | Medical Application |
|--------------------------|-----------|-----------------------------------------------|--------------------|-------------------------------------------|
| ^{225}Ac | 9.92 d | $^{232}\text{Th}(\text{p}, \text{x})$ | 60-80 | TAT ¹ |
| ^{155}Tb | 5.32 d | $^{159}\text{Tb}(\text{p}, 5\text{n})$ | 40-60 | SPECT ² |
| ^{149}Tb | 4.12 h | $^{154}\text{Gd}(\text{p}, 6\text{n})$ | 70-80 | TAT, SPECT |
| ^{125}I | 59.41 d | $^{126}\text{Te}(\text{p}, 2\text{n})$ | 10-30 | SPECT |
| ^{103}Pd | 16.99 d | $^{103}\text{Rh}(\text{p}, \text{n})$ | 10-20 | AT ³ |
| $^{99\text{m}}\text{Tc}$ | 6.01 h | $^{100}\text{Mo}(\text{p}, 2\text{n})$ | 20-80 | SPECT |
| ^{89}Zr | 78.41 h | $^{89}\text{Y}(\text{p}, \text{x})$ | 10-20 | PET ⁴ |
| ^{86}Y | 14.74 h | $^{88}\text{Sr}(\text{p}, 3\text{n})$ | 30-80 | PET |
| ^{82}Sr | 25.35 d | $^{\text{nat}}\text{Rb}(\text{p}, \text{xn})$ | 40-80 | $^{82}\text{Sr}/^{82}\text{Rb}$ Generator |
| ^{75}Se | 7.15 h | $^{75}\text{As}(\text{p}, 3\text{n})$ | 30-50 | PET |
| ^{68}Ge | 270.93 d | $^{\text{nat}}\text{Ga}(\text{p}, \text{x})$ | 20-80 | $^{68}\text{Ge}/^{68}\text{Ga}$ Generator |
| ^{62}Zn | 9.19 h | $^{\text{nat}}\text{Cu}(\text{p}, \text{x})$ | 10-40 | PET |

¹ TAT: Targeted Alpha Therapy² SPECT: Single Photon Emission Computed Tomography³ AT: Auger Electron Therapy⁴ PET: Positron Emission Computed Tomography

After the upgrade of CSNS-II, which will be complete in 2028, the maximum proton energy of the APEP line is expected to reach 300 MeV with a proton beam current of approximately 333.3 μA (see in **Table 1**), significantly extending the variety of isotopes which can be produced. To fully utilize the proton energy, isotopes of interest are expected to be generated by spallation (p, x) reactions at the 300-MeV APEP. High-energy protons can produce isotopes with a wide range of masses, providing an opportunity to study rare radioisotopes. Considering the cross section of the production reaction and the impurity content, appropriate target materials are essential for the generation of nuclides with different mass numbers. **Table 3** lists the potential medical isotopes produced by the 300-MeV proton beam. Irradiation of thorium or tantalum target with 300-MeV protons can produce a series of products, including some crucial alpha-emitter isotopes and lanthanide isotopes, which are ideal isotopes for medical applications.

Table 3. Potential medical isotopes that can be produced by the 300 MeV proton beam. (CSNS-II, APEP).

| Medical Isotope | Half-Life | Reaction Channel | Proton Energy(MeV) | Medical Application |
|-------------------|-----------|------------------------------------------------------------|--------------------|---------------------|
| ^{225}Ac | 9.92 d | $^{232}\text{Th}(\text{p, x})/^{238}\text{U}(\text{p, x})$ | 300 | TAT |
| ^{223}Ra | 11.43 d | $^{232}\text{Th}(\text{p, x})/^{238}\text{U}(\text{p, x})$ | 300 | TAT |
| ^{213}Bi | 45.59 m | Decay from ^{225}Ac | 300 | TAT |
| ^{177}Lu | 6.64 d | $^{181}\text{Ta}(\text{p, x})$ | 300 | β Therapy |
| ^{173}Lu | 1.37 y | $^{181}\text{Ta}(\text{p, x})$ | 300 | β Therapy |
| ^{166}Yb | 56.71 h | $^{181}\text{Ta}(\text{p, x})$ | 300 | AT |
| ^{169}Yb | 32.02 d | $^{181}\text{Ta}(\text{p, x})$ | 300 | SPECT |
| ^{149}Tb | 4.12 h | $^{181}\text{Ta}(\text{p, x})$ | 300 | TAT, SPECT |
| ^{155}Tb | 5.32 d | $^{181}\text{Ta}(\text{p, x})$ | 300 | SPECT |
| ^{140}Nd | 3.37 d | $^{181}\text{Ta}(\text{p, x})$ | 300 | AT, PET |
| ^{85}Sr | 64.85 d | $^{89}\text{Y}(\text{p, x})$ | 300 | SPECT |
| ^{83}Rb | 86.21 d | $^{89}\text{Y}(\text{p, x})$ | 300 | SPECT |

3. Simulation

3.1 Simulation code

Several codes are able to accurately simulate the passage of particles through matter, such as FLUKA^[23] and GEANT4^[24]. FLUKA was employed in this study owing to its convenient information extraction features and abundant reaction cross-section libraries. The proton reaction cross-section data from the code are parameterized based on the primary energy and target nucleus, rather than relying on an integrated cross-section channel-by-channel. Based on existing experimental results and simulation experience at APEP, the isotope production rates calculated using FLUKA theoretical cross-sections can provide reliable guidance for experiments^{[7][22][25]}. The functions implemented in the code facilitate the acquisition of the parameters of the proton-induced nuclear reaction, such as the types of reaction products, decay of radioactive isotopes, and induced radioactivity resulting from nuclear interactions. In the FLUKA simulation, the coalescence process and a new fragmentation model were activated, which are critical for the calculation of residual nuclei. The generation and transport of decay radiation are embedded in the code because a dedicated database of decay emissions based mostly on information obtained from the NNDC is used^[23]. To investigate the in-target activity of the isotopes as a function of irradiation time, the following decay law has been embedded into the code,

$$\frac{dN_i(t)}{dt} = \lambda_{p \rightarrow i} N_p(t) + R_{T \rightarrow i} N_T(t) - \lambda_i N_i(t), \quad (1)$$

where N_i, N_p, N_T represent the number of the produced isotope, parent isotope and target isotope, respectively. $\lambda_{p \rightarrow i}$ and λ_i represent the decay constant of the parent isotope and produced isotope. The first term on the right side is the contribution from the decay of the parent nucleus, the second term is the contribution from the nuclear reaction of protons with the irradiation target, and the third term is the loss term, indicating the decay of the produced isotope itself. Using FLUKA, we obtained results for the production of residuals, their time evolution, and residual doses owing to their decays in the simulation. These procedures ensure qualified simulation results for the yield of radioisotopes produced by the proton beams at the CSNS.

3.2 Simulation method

To analyze the feasibility of isotope production based on proton beams at the CSNS, simulations of the reaction processes were performed to determine the activities of different isotopes under particular circumstances. The thickness and density of the irradiation targets are considered as uniform. The isotope abundance for the target material is considered in the simulation while the impurity is ignored. In practice, the experimental activity generated in the target may be lower than the simulated result, and the proportions of the product species differ slightly between the experiment and simulation because of the presence of impurities in the target materials. The irradiated target geometry was a solid cylinder, composed entirely of the target material. The diameter of the targets was 2 cm, as determined by the beam spot size of the APEP (2 cm \times 2 cm). For targets made of different materials, the proton utilization rate was improved by adjusting the target thickness in the simulation, ensuring that the proton energy was fully deposited on the targets. In the simulation, the protons vertically incident on the target and produced a series of isotopes by interacting with the target nucleus. The parameters of interest, such as proton number Z, neutron number N, and mass number A of all products, were acquired and recorded during the simulation. The influence of secondary particles generated by proton bombardment, including neutrons and gamma-rays, on the simulated yield was also considered. The results are discussed in detail in the following section.

3.3 Alternative targets

The selection of target materials depends on their physical and chemical properties as well as the impurities produced by the reaction with protons. The fabrication technique for the irradiation targets is not discussed in this paper. This study focused on the physical analysis of proton reactions with different target materials, including the activities of radioisotopes and their corresponding impurities, as well as the influence of various factors on purity.

Table 4 lists the alternative target materials expected for isotope production at CSNS. Several reaction channels can be used to produce medical isotopes, such as the proton-induced (p, x) , (p, n) , $(p, 2n)$ reactions. The proton-induced (p, x) reaction can generate isotopes with a wide range of mass numbers. However, the cross section of (p, x) reaction is small, and the separation of isotopes is difficult due to the large number of nuclides produced. Some classic medical isotopes can also be produced by (p, n) , $(p, 2n)$ or other reactions with lower energy and higher cross section, whereas the irradiation target materials must be particularly designed for specific isotopes produced by these reactions. Generally, single reaction channels such as (p, n) and $(p, 2n)$ exhibit resonance energies, where the reaction cross section reaches its maximum, as listed in **Table 4**. However, for the (p, x) reaction, there is no distinct resonance peak due to the combined effects of multiple reaction channels. It should be noted that the isotopes listed in the table are accompanied by the production of a large amount of impurities, so detailed impurity analysis must be conducted for specific isotopes before production. In particular, the medical isotopes generated through (p, x) reaction of the 300 MeV proton are accompanied by the simultaneous production of hundreds of impurities, making subsequent chemical separation of isotopes a significant challenge.

As listed in **Table 4**, the ideal target materials for spallation reactions include uranium, thorium, tantalum, yttrium, and titanium. These materials are not prohibitively radioactive, induce fewer radiological hazards, and are readily available as target materials. The ability of existing facilities and methods to fabricate, irradiate, and process these targets has been demonstrated [26][27]. Considering the difficulty in target fabrication and the counting limitations of high-purity germanium detectors, we recommend selecting the target thicknesses between 100 μm and 1 mm for verification experiments. At CSNS-II, the alpha-emitter radioisotopes ^{225}Ac is expected to be

produced using a thorium target, which is the interested radioisotope at the 300-MeV APEP due to the high proton energy of APEP and the urgent demand for ^{225}Ac in the domestic market.

Table 4. Typical targets for isotope production by the proton beams at CSNS APEP.

| Target nucleus | Target composition | Medical isotopes | Reaction channels | Resonance (Irradiation) energy (MeV) |
|-------------------|-------------------------------------------------|-----------------------------------------------------------------------------------------------------------------------|-------------------|--------------------------------------|
| ^{232}Th | ThO_2 or ^{232}Th metal | ^{225}Ac , ^{223}Ra | (p, x) | 300 |
| ^{181}Ta | ^{181}Ta metal | ^{177}Lu , ^{169}Yb , ^{166}Yb , ^{166}Ho , ^{152}Tb , ^{140}Nd | (p, x) | 300 |
| ^{89}Y | Y_2O_3 or ^{89}Y metal | ^{85}Sr , ^{83}Rb , ^{74}As | (p, x) | 300 |
| ^{48}Ti | Natural Ti or ^{48}Ti metal | ^{44}Sc , ^{47}Sc | (p, x) | 300 |
| ^{159}Tb | ^{159}Tb metal | ^{155}Tb | (p, x) | 300 |
| ^{165}Ho | ^{165}Ho metal | ^{165}Er | (p, n) | 9-10 |
| ^{103}Rh | ^{103}Rh metal | ^{103}Pd | (p, n) | 9-10 |
| ^{100}Mo | Natural Mo or ^{100}Mo metal | $^{99\text{m}}\text{Tc}$ | (p, 2n) | 15-20 |
| ^{124}Te | ^{124}Te metal | ^{123}I | (p, 2n) | 20-25 |
| ^{88}Sr | ^{88}Sr metal | ^{86}Y | (p, 3n) | 35-40 |
| ^{75}As | Natural As | ^{73}Se | (p, 3n) | 30-35 |
| ^{154}Gd | ^{154}Gd metal | ^{149}Tb | (p, 6n) | 35-40 |

4. Analysis of recommended radioisotopes for production at CSNS-II

Radiologic diagnosis and therapy utilize various types of radioactive emissions to image or kill cancer cells, including gamma (γ), alpha (α), beta (β^- and β^+), and Auger electron. Diagnostic procedures using radioisotopes are now routine, and the gamma- and positron-emitting radionuclides are extensively used in diagnosis (e.g., $^{99\text{m}}\text{Tc}$ (γ -emitter) and ^{18}F (β^+ -emitter)) [22][28]. Alpha emitter radioisotopes such as ^{225}Ac , ^{223}Ra , and ^{211}At are becoming more interested in targeted α therapy [29]-[31]. β^- radioisotopes have been applied in clinical practice, including ^{90}Y and ^{177}Lu [32][33]. Auger electron-emitting radioisotopes such as ^{165}Er and ^{67}Ga are also being considered for targeted therapy [11][34].

In this section, the recommended radioisotopes for research and production at the CSNS are discussed. Analysis of all potential irradiation targets and corresponding isotopes that could be produced at the CSNS is beyond the scope of this study. We focus on several medical radioisotopes with significant applications that are either promising or extensively used in the medical field. The types of radioisotopes that can be produced by the 300-MeV proton beam of CSNS-II are of great concern to us because of the high proton intensity and production capacity.

4.1 Alpha-emitting radioisotopes

Targeted Alpha Therapy (TAT) is one of the most promising tumor therapies for the future, and the development of radiopharmaceuticals emitting alpha ions is an active field of academic and commercial research worldwide^[35]. Alpha radiation can kill cancer cells that are resistant to treatment with beta- or gamma irradiation as well as chemotherapeutic drugs. Additionally, alpha radiation has a shorter range in tissue than beta or gamma radiation, which reduces the risk of damaging surrounding healthy tissue. Generally, the range of α - particles in tissue is 50-100 μm , and they have high linear energy transfer (LET) with a mean energy deposition of 100 keV/ μm , which provides a more specific tumor cell killing ability without damage to the surrounding normal tissues than β^- particles^[36]. Only a few alpha-emitting radioisotopes can be suitable for the TAT therapy, including ^{225}Ac , ^{223}Ra , $^{212,213}\text{Bi}$, and ^{211}At . These candidate radioisotopes with suitable half-lives have favorable properties for cancer therapy, as detailed in the following subsections.

4.1.1 $^{225}\text{Ac}/^{213}\text{Bi}$

Actinium-225 (^{225}Ac) has become increasingly prominent owing to its suitable half-life ($T_{1/2} = 9.9$ d) and short range in tissues. The long half-life of ^{225}Ac allows slow decay during production and delivery. The alpha particles released by ^{225}Ac have a high LET and a short range of about 50-90 μm in biological tissue, which are conducive to killing tumor cells effectively and minimizing damage to normal tissues. However, the application of ^{225}Ac -radiopharmaceutical still faces significant challenges, including limited isotope supply and difficulty in chemical separation. Four main different routes are proposed to produce ^{225}Ac : (1) decay from the ^{229}Th sources; (2) (p , $2n$) reaction of ^{226}Ra with the proton energy above about 16 MeV; (3) (p , x) reaction of ^{232}Th (^{238}U) via high-energy protons; (4) (γ , n) reaction of ^{226}Ra produces ^{225}Ra , which subsequently decays to ^{225}Ac . More details can be found in the literature^{[10][35][37]}. At CSNS, the last route is recommended to perform the experiment of the ^{225}Ac production due to the high proton energy and the adept ^{232}Th target-making technique of the researchers. Based on our previous experience, ^{232}Th targets can be prepared using either cold- or hot- pressing with ^{232}Th metal powder, depending on the required thickness^{[38][39]}. By comparing the existing cross-sectional data of ^{232}Th (p , x) reaction at different energies^[40], we found that the 300-MeV proton beam is very suitable for the production of ^{225}Ac .

Figure 2 shows the generation and decay schemes for ^{225}Ac and ^{213}Bi . ^{225}Ac is produced through proton-induced spallation of ^{232}Th , followed by the decay of 3 α -particles to ^{213}Bi , which is another important medical alpha-emitting radionuclide.

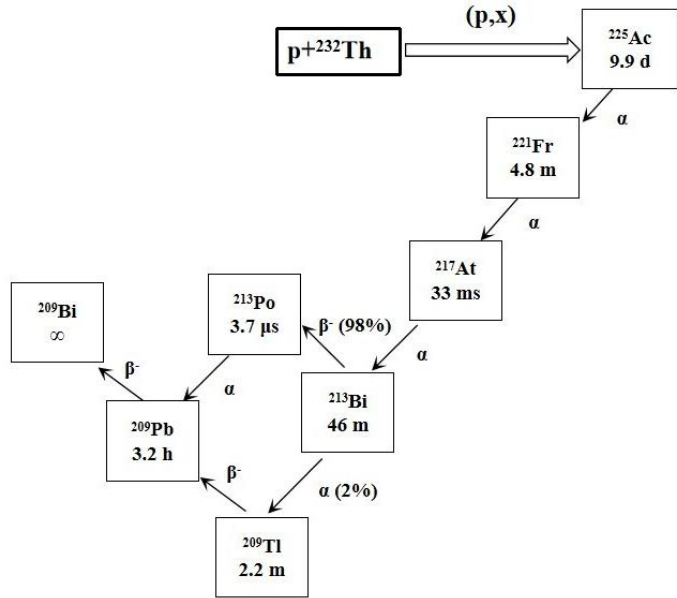


Fig.2. Generation and decay scheme of ^{225}Ac to ^{213}Bi .

To evaluate the in-target production rate, the reaction process between 300-MeV protons and ^{232}Th was simulated using the FLUKA code, with the geometric model described in **Section 3.2**. The beam intensity was set to $333.3 \mu\text{A}$ based on the design parameters of CSNS-II. The thickness of ^{232}Th target was evaluated using the SRIM code^[41] to ensure full deposition of proton energy in the target, which was used as an input for FLUKA. The irradiation time was set to 6 d, which was determined by the operational status of the CSNS. Several important parameters, including the weekly production activity of ^{225}Ac , the evolution of activity over time, and the radionuclidian impurities of ^{225}Ac , are discussed.

The activity evolution of the main isotopes of ^{225}Ac in the irradiated thorium target with a 10 cm thickness is shown in **Figure 3**. The activity of ^{225}Ac increased to approximately 57 Ci after a 6-d irradiation with no off time, which indicates that CSNS-II APEP is capable of producing 1710 Ci ^{225}Ac per year during 30 weeks of annual operation time with dedicated irradiation. **Figure 3 (a)** shows that the impurity ratio of ^{227}Ac increased with irradiation time. The $^{227}\text{Ac}/^{225}\text{Ac}$ ratio was 0.146% after 6 d of irradiation and increased to 0.216% after continuous irradiation for 20 d. After irradiation for a certain period (6 d), the irradiation target was removed in a timely manner and

subjected to chemical separation. Based on the results in **Fig. 3(b)**, it can be observed that the ratio of ^{225}Ac activity to the total activity reaches its peak when the cooling time is approximately 10–20 d, which can be used to estimate the optimal cooling time in practical production.

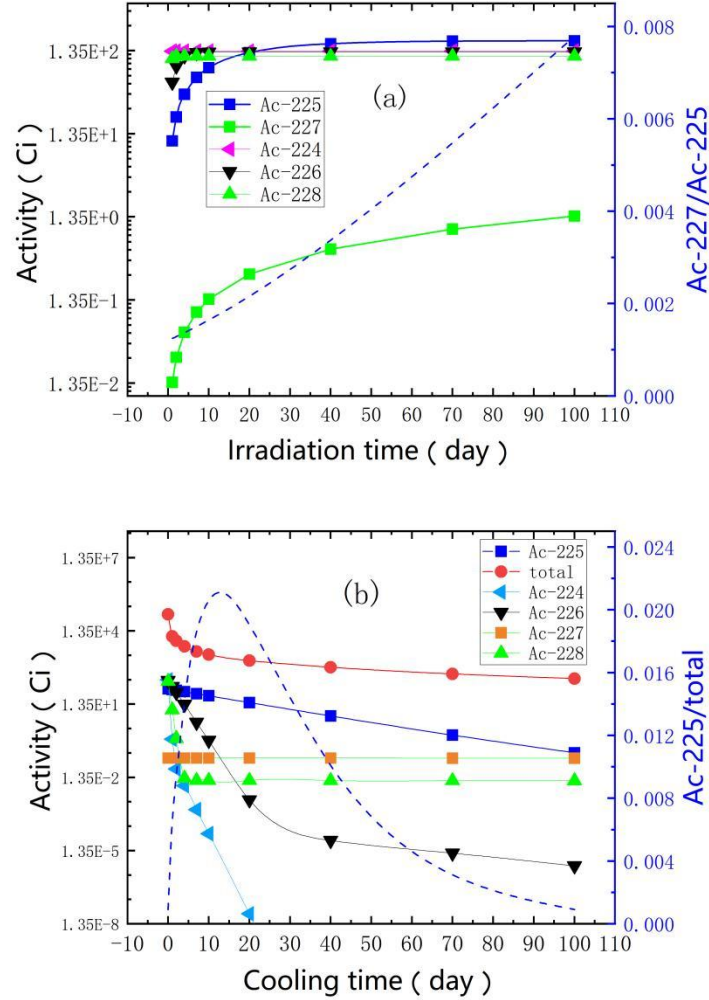


Fig.3. ^{225}Ac activity evolution with irradiation time (a) and cooling time (b) in the irradiated thorium target (thickness = 10 cm), accompanying with the activity evolution of major impurities. The dashed lines represent the ratios of $^{227}\text{Ac}/^{225}\text{Ac}$ (a) and $^{225}\text{Ac}/$ total (b) activity, with the corresponding values on the right axes. Note that (b) corresponds to an irradiation time of 6 d.

From **Figure 2**, one can see that the short-lived daughter nuclide, ^{213}Bi ($T_{1/2} = 46$ min), is obtained by the emission of three α -particles from ^{225}Ac and subsequently undergoes alpha-decay and beta-decay to produce ^{209}Tl (2%) and ^{213}Po (98%), respectively, with an α energy of about 8.4 MeV and a short tissue range of about 85 μm . ^{213}Bi is a promising alpha-emitting radioisotope for

application in TAT and can be conveniently produced using a ^{225}Ac - ^{213}Bi generator with high specific activity. Detailed descriptions of ^{213}Bi are provided in [36][42][43]. The information depicted in **Figure 4** reveals that the production yield of ^{213}Bi is nearly equivalent to that of ^{225}Ac , primarily because of the notably longer half-life of ^{225}Ac in that of ^{213}Bi . The simulation results showed that the CSNS could provide a substantial amount of ^{225}Ac and ^{213}Bi for drug research and clinical studies.

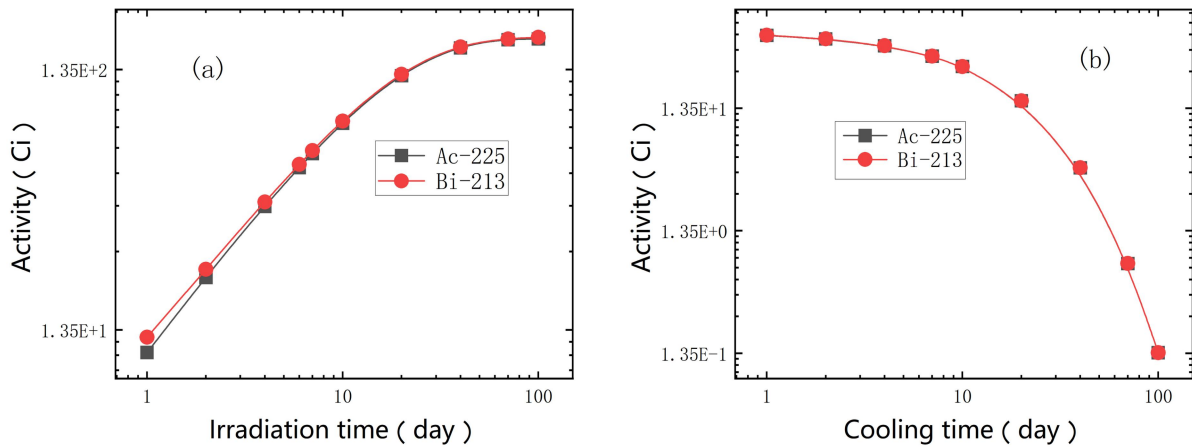


Fig.4. Evolution of ^{213}Bi activity with irradiation time (a) and cooling time (b) in the irradiated thorium target (thickness = 10 cm), accompanying with the activity evolution of ^{225}Ac . Note that (b) corresponds to an irradiation time of 6 d.

4.1.2 ^{223}Ra

^{223}Ra ($T_{1/2} = 11.4$ d) is considered one of the most promising alpha-emitting radioisotopes based on its decay characteristics. The long half-life of ^{223}Ra allows ample time for transportation, drug preparation, and injection into patients. As a bone-seeking radiopharmaceutical, Xofigo ($^{223}\text{RaCl}_2$) has been used in the clinical treatment of skeletal metastases from breast and prostate cancers [44]-[46], and is the first TAT radiopharmaceutical worldwide.

In CSNS-II, the production of ^{223}Ra is also expected by employing ^{232}Th as the target nucleus. As shown in **Figure 5**, the spallation reaction produced by the protons on thorium can directly produce ^{223}Ra , and the ^{223}Ra can also be formed by the decay of ^{227}Th and ^{227}Ac which are simultaneously produced by the spallation reactions. Subsequently, ^{223}Ra decays into a stable lead through a series of short-lived daughter radionuclides, emitting four alpha particles. In the decay

chain of ^{223}Ra , 94% of the total decay energy is released by alpha particles [44], indicating that cancer cells can be effectively killed.

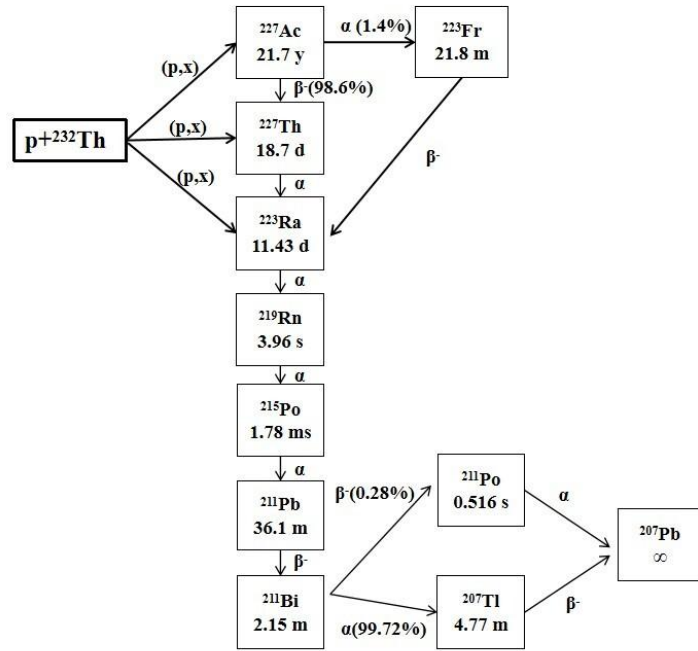


Fig.5. Generation and decay scheme of ^{223}Ra .

^{223}Ra can also be generated from $^{227}\text{Ac}/^{227}\text{Th}$ and purified using Ac-resin, which immobilizes both ^{227}Ac and ^{227}Th , as previously described [44]. **Figure 6** illustrates the variation in radioactive activity with irradiation and cooling times for the three nuclides. As shown in **Figure 6**, the EOB activity corresponding to one week of irradiation was approximately 14.5 Ci. However, with an increase in the cooling time, ^{227}Ac and ^{227}Th produced by the spallation reaction continued to decay to ^{223}Ra , resulting in an increase in ^{223}Ra production. After cooling for approximately 20 d, ^{223}Ra reached a maximum activity of approximately 24 Ci and maintained a relatively high yield for a long time, which provided sufficient time for chemical separation.

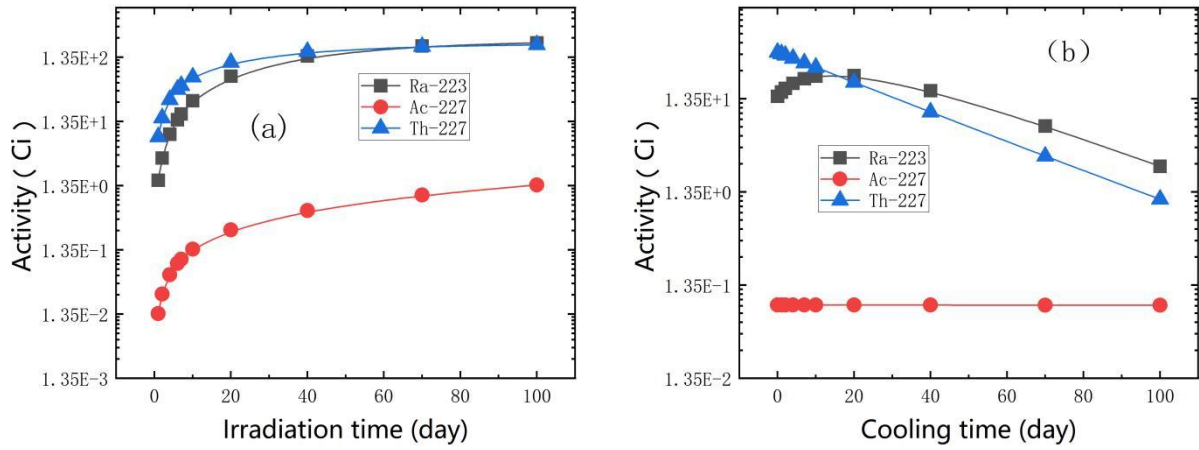


Fig.6. Evolution of ^{223}Ra activity with irradiation time (a) and cooling time (b) in the irradiated thorium target (thickness = 10 cm), accompanying with the activity evolution of ^{227}Ac and ^{227}Th . Note that (b) corresponds to an irradiation time of 6 d.

4.1.3 ^{211}At

^{211}At also has attracted significant attention as a therapeutic α -particle emitter for its promising potential in treating microscopic diseases, such as micrometastases and monocellular malignancies [47][48]. Typically, ^{211}At ($T_{1/2} = 7.2$ h) is more suitable for production by alpha accelerators based on the ^{209}Bi (α , $2n$) reaction with a cross section value of ~ 1 b at $E_\alpha = 29$ MeV[49]. However, this restricts the production of ^{211}At owing to the limited number of alpha accelerators available worldwide.

Recently, researchers have discovered that the use of high-energy protons to bombard Th or U targets to produce ^{211}Rn ($T_{1/2} = 14.6$ h), the mother isotope of ^{211}At , is an attractive pathway for producing ^{211}At [49]. A $^{211}\text{Rn}/^{211}\text{At}$ generator system is recommended for producing ^{211}At . As shown in **Figure 7**, at CSNS-II, ^{211}At and ^{211}Rn can be generated through proton irradiation of thorium. Simultaneously, ^{211}At is produced via the electron capture (EC) decay of ^{211}Rn with a probability of approximately 73%. Subsequently, ^{211}At decays into ^{207}Bi and ^{211}Po through the α decay (42%) and EC decay (58%), respectively.

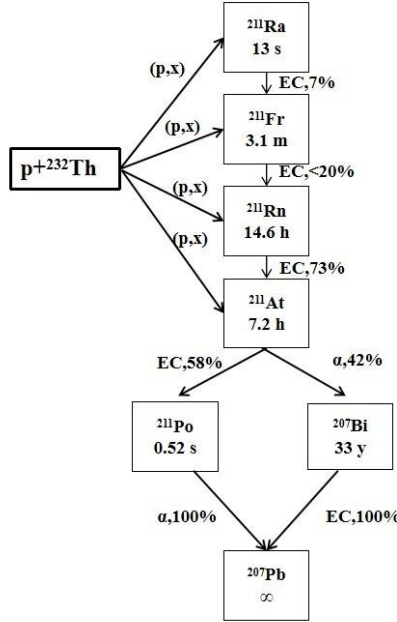


Fig.7. Generation and decay scheme of ^{211}At .

The activity evolutions of ^{211}At and ^{211}Rn were calculated, and the results are shown in **Figure 8**. The irradiation of thorium target for 6 d with a proton beam intensity of $333.3 \mu\text{A}$ can produce a maximum of approximately 163.5 Ci of ^{211}At . However, because of the short half-life of ^{211}At , the activity reaches the maximum value quickly, which means that prolonged irradiation does not effectively increase the yield (**Fig. 8 (a)**), and frequent irradiation can improve the production yield.

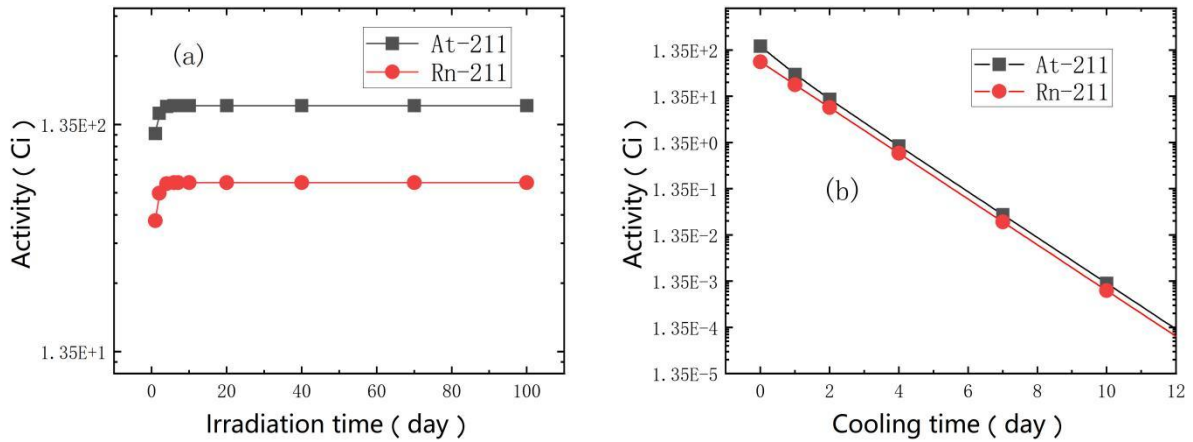


Fig.8. Evolution of ^{211}At activity with irradiation time (a) and cooling time (b) in the irradiated thorium target (thickness = 10 cm), accompanying with the activity evolution of ^{211}Rn . Note that (b) corresponds to an irradiation time of 6 d.

Other alpha-emitting isotopes, such as ^{212}Pb and ^{212}Bi , which are potential candidates for TAT, may not be optimally produced by proton accelerator irradiation. However, we discovered that a considerable in-target yield of these isotopes could also be obtained using thorium as the irradiation target at CSNS-II, which is adequate for proof-of-principle studies and pre-clinical drug research. The weekly production yields of these isotopes and the aforementioned categories are listed in **Table 5**. Currently, two main methods are used for separating alpha-emitting isotopes based on thorium targets. Taking the separation of ^{225}Ac as an example, a three-step procedure including liquid-liquid and solid-phase extraction chromatography can result in a recovery rate of over 85% for ^{225}Ac [50]. A two-step method using 1 M oxalic acid at pH 2 to remove the bulk thorium mass can yield ^{225}Ac with a recovery yield of over 98%, which is suitable for radiolabeling or generator applications [51][52]. In addition, alpha-emitting radioisotopes can be separated using an on-line isotope separation method according to their mass-to-charge ratio. Based on the existing experiences of CERN MEDICIS (2.0 GeV, 6.7 uA)^[9] and TRIUMF ISAC (500 MeV, 100 uA)^[11], CSNS APEP (300 MeV, 333.3 uA) has the potential to provide sufficient yields for clinical experiments by the on-line isotope separation method. In summary, the 300 MeV proton beam at CSNS-II is very suitable for the production of alpha-emitting isotopes and provides an excellent experimental platform for isotope production.

Table 5. In-target production yield of alpha-emitter radioisotopes at CSNS-II

| Medical Isotope | Energy of α (MeV) | Production pathway | Theoretical yield (Ci/week, 100 kW) | Daughter isotopes |
|-------------------|--------------------------|--------------------|-------------------------------------|-----------------------------------------------------------------------------------------------------------------------|
| ^{211}At | 5.9 | | 163.5 | ^{211}Po 、 ^{207}Bi |
| ^{212}Bi | 6.1 | | 103.0 | ^{212}Po 、 ^{208}Tl |
| ^{212}Pb | 6.1 | Accelerator | 89.5 | ^{212}Bi 、 ^{212}Po 、 ^{208}Tl |
| ^{213}Bi | 5.8 | irradiation | 58.5 | ^{213}Po 、 ^{209}Tl 、 ^{209}Pb |
| ^{225}Ac | 5.8 | | 57.0 | ^{221}Fr 、 ^{217}At 、 ^{213}Bi 、 ^{213}Po 、 ^{209}Tl 、 ^{209}Pb |
| ^{223}Ra | 5.7 | | 14.5 | ^{219}Rn 、 ^{215}Po 、 ^{211}Pb 、 ^{211}Bi 、 ^{211}Po 、 ^{207}Tl |

4.2 Neutron-deficient lanthanide isotopes

The following advantages make lanthanide radionuclides highly favorable : (1) lanthanide isotopes can emit different types of particles and possess all radiation characteristics suitable for

radiotherapy and diagnosis; (2) different lanthanide isotopes have similar chemical properties that provide unique advantages for the molecular labeling of tracer molecules. Neutron-rich lanthanide nuclides, such as ^{141}Ce , ^{143}Pr , and ^{153}Sm , are typically produced by bombarding ^{238}U with high-energy protons. Neutron-deficient lanthanide isotopes, such as ^{169}Yb , ^{167}Tm , ^{149}Tb , and ^{152}Tb , can be produced by bombarding a tantalum target.

In this study, the evolution of various neutron-deficient lanthanide radioisotopes suitable for production on CSNS-II was evaluated using the FLUKA code, with ^{181}Ta used as the target material. The tantalum target was bombarded by a 300 MeV proton beam with a power of 100 kW and an irradiation time of 6 d. To obtain the maximum in-target production yield, the thickness of the Ta target (8 cm) was maintained such that the proton energy was completely deposited on the target.

Figure 9 shows the variation trends of some lanthanide isotopes over time, and the specific weekly yields are summarized in **Table 6**. Several isotopes listed in the table have already been used in clinical therapy, and others are undergoing pre-clinical research but show promising application prospects. Lanthanide isotopes release different types of particles during radiotherapy or diagnosis. For example, ^{177}Lu has been used for beta therapy, ^{149}Tb for alpha therapy, and ^{152}Tb for PET. ^{165}Er is a promising candidate for Auger electron therapy, and ^{169}Yb is commonly used for SPECT.

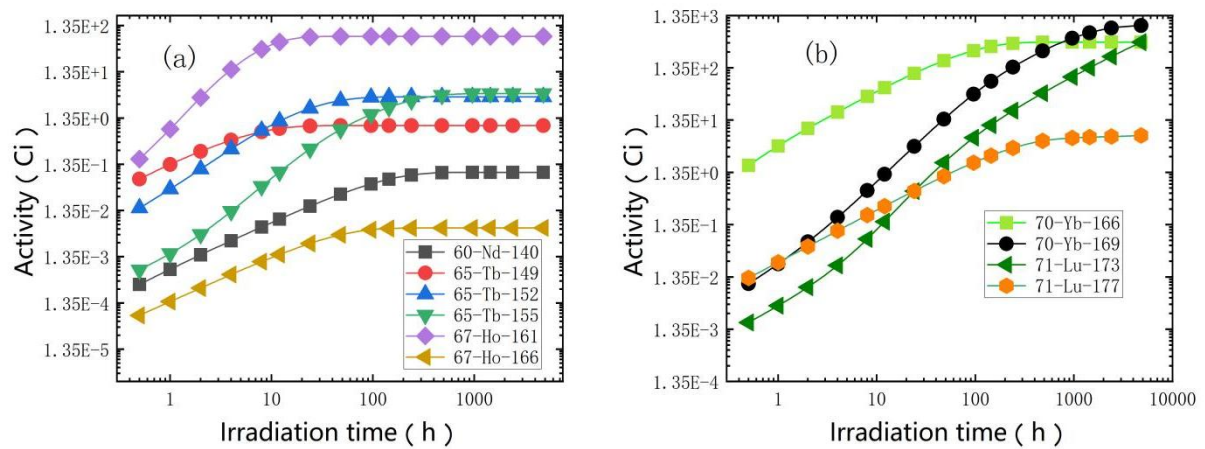


Fig.9. Evolution of the activity of lanthanide isotopes with irradiation time in the irradiated tantalum target (thickness = 8 cm).

Table 6. In-target production yield of neutron-deficient lanthanide isotopes at CSNS-II

| Medical isotopes | Theoretical yield (100 kW, Ci/week) | Decay modes | Daughter isotopes |
|-------------------|----------------------------------------|----------------|---------------------------------------|
| ^{166}Yb | 343.0 | EC | ^{166}Tm 、 ^{166}Er |
| ^{165}Er | 277.0 | EC | ^{165}Ho |

| | | | |
|-------------------|-------|---------------|--------------------------------------------------------------------------------------------------------------------------------------------------------|
| ¹⁶⁷ Tm | 188.0 | EC | ¹⁶⁷ Er |
| ¹⁶¹ Ho | 78.5 | EC | ¹⁶¹ Dy, ¹⁵⁷ Gd |
| ¹⁶⁹ Yb | 74.5 | EC | ¹⁶⁹ Tm |
| ¹⁵² Tb | 3.9 | EC, β^+ | ¹⁵² Gd, ¹⁴⁸ Eu, ¹⁴⁸ Sm, ¹⁴⁴ Nd, ¹⁴⁰ Ce, ¹⁴⁴ Pm |
| ¹⁷⁷ Lu | 2.8 | β^- | ¹⁷⁷ Hf |
| ¹⁵⁵ Tb | 2.4 | EC | ¹⁵⁵ Gd |
| ¹⁴⁹ Tb | 0.9 | EC, β^+ | ¹⁴⁹ Gd, ¹⁴⁵ Eu, ¹⁴⁹ Eu, ¹⁴⁹ Sm, ¹⁴⁵ Sm, ¹⁴⁵ Pm, ¹⁴⁵ Nd, ¹⁴¹ Pr |
| ¹⁴⁹ Gd | 0.5 | EC, β^+ | ¹⁴⁹ Eu, ¹⁴⁹ Sm, ¹⁴⁵ Sm, ¹⁴⁵ Pm, ¹⁴⁵ Nd, ¹⁴¹ Pr |

As shown in **Table 6**, a wide range of lanthanide isotopes can be obtained by reacting protons with tantalum; however, some of these can be produced in higher yields using other irradiation targets and reaction channels. Hence, our preference was to utilize the CSNS for the centralized production of one or a few medical radioisotopes, such as the previously mentioned ²²⁵Ac. For other isotopes, we are committed to providing adequate quantities for verification rather than for large-scale production.

4.3 Other medical radioisotopes

In addition to the alpha and lanthanide isotopes, we explored the feasibility of using other materials as irradiation targets to produce medical isotopes. Based on the principles of selecting the target materials mentioned in Section 3.3, some stable and naturally abundant isotopes, such as Y and Ti, can be chosen as target nuclei. The theoretical weekly yields of isotopes generated from the reaction of these targets with the 300-MeV proton beam were evaluated using FLUKA, and the results are listed in **Table 7**. The availability of these data can serve as a valuable reference for future research and can significantly broaden the range of medical isotopes that can be studied at CSNS-II.

Table 7. In-target production yield of other medical radioisotopes at CSNS-II

| Medical isotopes | Irradiation target | Half-life | Medical Application | Theoretical yield (100 kW, Ci/week) |
|------------------|--------------------|-----------|------------------------|-------------------------------------|
| ⁴⁴ Sc | ^{nat} Ti | 3.97 h | PET | 1131.0 |
| ⁴⁷ Sc | ^{nat} Ti | 3.4 d | β Therapy, SPECT | 629.5 |
| ⁸⁹ Zr | ⁸⁹ Y | 78.41 h | PET | 109.0 |
| ⁸⁵ Sr | ⁸⁹ Y | 64.85 d | SPECT | 105.5 |
| ⁸³ Rb | ⁸⁹ Y | 86.2 d | SPECT | 50.0 |
| ⁷² As | ⁸⁹ Y | 26.0 h | PET | 31.5 |
| ⁷¹ As | ⁸⁹ Y | 65.33 h | PET | 17.5 |

| | | | | |
|------------------|-----------------|--------|-----|-----|
| ⁷⁴ As | ⁸⁹ Y | 17.8 d | PET | 3.0 |
|------------------|-----------------|--------|-----|-----|

4.4 Ongoing research

The next focus of radioisotope research at the CSNS will be the production and separation of alpha-emitter radioisotopes. As described in Section 4.1.1, the unique radioactive properties of alpha-emitter radioisotopes make them particularly advantageous for cancer treatment and their supply has become a major issue in international commercial applications and academic research. Fortunately, the 300-MeV and 100-kW proton beam at CSNS-II provide ideal conditions for studying these nuclides in China. The spallation reaction of high-energy protons with different targets can produce a large number of rare nuclides, offering a unique opportunity for the study and collection of pre-clinical and, in some cases, clinical quantities of innovative medical radioisotopes. To fully utilize the CSNS beam, an irradiation program related to the production of ²²⁵Ac, including the physical design of the irradiation target, thermal analysis, and impurity analysis, is in progress.

5. Conclusion

In this study, the feasibility of isotope production using a CSNS proton beam was evaluated. Using the FLUKA code, the types and yields of medical isotopes produced by the proton beam at the CSNS were analyzed. The results show that the CSNS APEP facility can provide a unique opportunity for the production of a wide range of medical radioisotopes, especially alpha-emitting radioisotopes. By utilizing specific target materials, APEP can generate sufficient quantities of the desired radioisotopes for researchers to carry out proof-of-principle experiments and even for commercial applications. ²²⁵Ac and ²²³Ra will become the key alpha-emitter medical radioisotopes studied at the CSNS owing to their urgent demand in the domestic market; therefore, the production and separation of these two isotopes will be the main focus of our next work. In the future, we would like to explore the possibility of using online methods to separate the residual nuclei. With future upgrades of the CSNS APEP facility, there are supplementary possibilities for expanding the variety of radioisotopes suitable for medical applications.

Acknowledgments

This study was supported by the National Natural Science Foundation of China (Project No. 12075135) and the China Postdoctoral Science Foundation (No. 2022M721908).

References:

- [1] Radioisotopes in medicine, World nuclear association website 389 (2022). <https://www.world-nuclear.org/information-library/non-power-nuclear-applications/radioisotopes-research/radioisotopes-in-medicine.aspx>.
- [2] X.D. Tan, X.X. Liu, H.Y. Shao, Healthy China 2030: a vision for health care. *Value Health Reg. News.* **12**, 112–114 (2017). <https://doi.org/10.1016/j.vhri.2017.04.001>
- [3] L.Chen, R.Yan, X.Z. Kang et al., Study on the production characteristics of ^{131}I and ^{90}Sr isotopes in a molten salt reactor. *Nucl. Sci. Tech.* **32**, 33 (2021). <https://doi.org/10.1007/s41365-021-00867-1>
- [4] C.G. Yu, X.H. Wang, C. Wu et al., Supply of I-131 in a 2MW molten salt reactor with different production methods. *Appl. Radiat. Isot.* **166**, 109350 (2020). <https://doi.org/10.1016/j.apradiso.2020.109350>
- [5] C.G. Yu, C.Y. Zou, C. Wu et al., Sustainable supply of ^{99}Mo source in a 2 MW molten salt reactor using low-enriched uranium. *Appl. Radiat. Isot.* **160**, 109134 (2020). <https://doi.org/10.1016/j.apradiso.2020.109134>
- [6] N. Liu, J. Gao, Y. Yang et al., The current situation and prospect of accelerator produced medical radioisotopes (in Chinese). *J. Isot.* **35**, 05 (2022). <https://doi.org/10.7538/tws.2022.youxian.015>
- [7] R. Han, Z. Q. Chen, G. Y. Tian et al., Study of Medical Radioisotopes Production by Accelerator Induced Reactions with FLUKA (in Chinese). *Nucl. Phys. Rev.* **4**, 913-917 (2020). <https://doi.org/10.11804/NuclPhysRev.37.2020025>
- [8] L. Ren, Y.C. Han, J.C. Zhang et al., Neutronics analysis of a stacked structure for a subcritical system with LEU solution driven by a D-T neutron source for ^{99}Mo production. *Nucl. Sci. Tech.* **32**, 123 (2021). <https://doi.org/10.1007/s41365-021-00968-x>
- [9] C. Duchemin, J.P. Ramos, T. Stora et al., CERN-MEDICIS: a review since commissioning in 2017. *Front. Med.* **8**, 693682 (2021). <https://doi.org/10.3389/fmed.2021.693682>
- [10] W. Luo, M. Bobeica, I. Gheorghe et al. Estimates for production of radioisotopes of medical interest at Extreme Light Infrastructure – Nuclear Physics facility. *Appl. Phys. B* **122**, 8 (2016). <https://doi.org/10.1007/s00340-015-6292-9>

- [11] D.E. Fiaccabrino, P. Kunz, V. Radchenko, Potential for production of medical radionuclides with on-line isotope separation at the ISAC facility at TRIUMF and particular discussion of the examples of ^{165}Er and ^{155}Tb . *Nucl. Med. Biol.* **94/95**, 81–91 (2021). <https://doi.org/10.1016/j.nucmedbio.2021.01.003>
- [12] T.J. Zhang, Z.G. Li, C.J. Chu, CYCIAE-100, a 100MeV H-cyclotron for RIB production. *Nucl. Instrum. Meth. B* **261**, 1027-1031 (2007). <https://doi.org/10.1016/j.nimb.2007.04.231>
- [13] T.J. Zhang, Y.L. Lv, S.M. Wei et al., Isotope production by the high current proton beam of CYCIAE-100. *Nucl. Instrum. Meth. B* **463**, 119-122 (2020). <https://doi.org/10.1016/j.nimb.2019.07.001>
- [14] J. Wei, H.S. Chen, Y.W. Chen et al., China Spallation Neutron Source: design, R&D, and outlook. *Nucl. Instrum. Meth. A* **600**, 10–13 (2009). <https://doi.org/10.1016/j.nima.2008.11.017>
- [15] J. Wei, S.N. Fu, J.Y. Tang et al., China Spallation Neutron Source - an overview of application prospects. *Chin. Phys. C* **33**, 1033 (2009). <https://doi.org/10.1088/1674-1137/33/11/021>
- [16] H.S. Chen, X.L. Wang, China's first pulsed neutron source. *Nat. Mater.* **15**, 689-691 (2016). <https://doi.org/10.1038/nmat4655>
- [17] S. Wang, Y.W. An, S.X. Fang et al., An overview of design for CSNS/RCS and beam transport. *Sci. China Phys. Mech. Astron.* **54**, 239-244 (2011). <https://doi.org/10.1007/s11433-011-4564-x>
- [18] F.W. Wang, T.J. Liang, W. Yin et al., Physical design of target station and neutron instruments for China Spallation Neutron Source. *Sci. China Phys. Mech. Astron.* **56**, 2410–2424 (2013). <https://doi.org/10.1007/s11433-013-5345-5>
- [19] J.Y. Tang, Q. An, J.B. Bai et al., Back-n white neutron source at CSNS and its applications. *Nucl. Sci. Tech.* **32**, 11 (2021). <https://doi.org/10.1007/s41365-021-00846-6>
- [20] Y.Y. Liu, H.T. Jing, L.S. Huang et al., Physical design of the APEP beam line at CSNS. *Nucl. Instrum. Meth. A* **1042**, 167431(2022). <https://doi.org/10.1016/j.nima.2022.167431>
- [21] G. Beyer, Radioactive ion beams for biomedical research and nuclear medical application. *Hyperfine Interact.* **129**, 529-553 (2000). <https://doi.org/10.1023/A:1012670018533>
- [22] Q.F. Dong, H.T. Jing, W.L. Li et al., Research on the production of $^{99\text{m}}\text{Tc}$ and ^{99}Mo using multi-layer targets at APEP. *Radiat. Phys. Chem.* **214**, 111287 (2024). <https://doi.org/10.1016/j.radphyschem.2023.111287>

- [23] G. Battistoni, F. Cerutti, A. Fasso et al., The FLUKA code: Description and benchmarking. AIP Conf. Proc. Am. Inst. Phys. **896**, 31-49 (2007). <https://doi.org/10.1063/1.2720455>
- [24] S. Agostinelli, J. Allison, K. Amako et al., GEANT4—a simulation toolkit. Nucl. Instrum. Methods Phys. Res. A **506**, 250-303 (2003). [https://doi.org/10.1016/S0168-9002\(03\)01368-8](https://doi.org/10.1016/S0168-9002(03)01368-8)
- [25] F.H. Garcia, C. Andreoiu, P. Kunz, Calculation of in-target production rates for isotope beam production at TRIUMF. Nucl. Instrum. Meth. B **412**, 174–179 (2017). <https://doi.org/10.1016/j.nimb.2017.09.023>
- [26] R. M. S. Augusto , L. Buehler , Z. Lawson et al., CERN-MEDICIS (Medical Isotopes Collected from ISOLDE): A new facility. Appl. Sci. **4**, 265-281 (2014). <https://doi.org/10.3390/app4020265>
- [27] P. Kunz, P. Bricault, M. Dombsky et al., Composite uranium carbide targets at TRIUMF: Development and characterization with SEM, XRD, XRF and L-edge densitometry. J. Nucl. Mater. **440**, 110-116 (2013). <https://doi.org/10.1016/j.jnucmat.2013.04.065>
- [28] E. Hess, G. Blessing, H.H. Coenen et al., Improved target system for production of high purity [¹⁸F]fluorine via the ¹⁸O(p, n)¹⁸F reaction. Appl. Radiat. Isot. **52**, 1431-1440 (2000). [https://doi.org/10.1016/S0969-8043\(99\)00248-1](https://doi.org/10.1016/S0969-8043(99)00248-1)
- [29] C. Kratochwil, F. Bruchertseifer, F.L. Giesel et al., ²²⁵Ac-PSMA-617 for PSMA-targeted α -radiation therapy of metastatic castration-resistant prostate cancer. J. Nucl. Med. **57**, 1941-1944 (2016). <https://doi.org/10.2967/jnumed.116.178673>
- [30] C. Parker, S. Nilsson, D. Heinrich et al., Alpha emitter radium-223 and survival in metastatic prostate cancer. N Engl J. Med. **369**, 213-223 (2013). <https://doi.org/10.1056/NEJMoa1213755>
- [31] J.R. Crawford, P. Kunz, H. Yang et al., ²¹¹Rn/²¹¹At and ²⁰⁹At production with intense mass separated Fr ion beams for preclinical ²¹¹At-based α -therapy research. Appl. Radiat. Isot. **122**, 222-228(2017).<https://doi.org/10.1016/j.apradiso.2017.01.035>
- [32] T. Tiwari, C. Malone, G. Foltz et al., Yttrium-90 radioembolization: current clinical practice and review of the recent literature. J. Radiol. Nurs. **38**, 86-91 (2019). <https://doi.org/10.1016/j.jradnu.2019.03.004>

- [33] B.L.R. Kam, J.J.M. Teunissen, E.P. Krenning et al., Lutetium-labelled peptides for therapy of neuroendocrine tumours. *Eur. J. Nucl. Med. Mol. Imag.* **39**, 103-112 (2012). <https://doi.org/10.1007/s00259-011-2039-y>
- [34] M. F. Othman, E. Verger, I. Costa et al., In vitro cytotoxicity of Auger electron-emitting [67Ga] Ga-trastuzumab. *Nucl. Med. Biol.* **80**, 57-64 (2020). <https://doi.org/10.1016/j.nucmedbio.2019.12.004>
- [35] A.K.H. Robertson, C.F. Ramogida, P. Schaffer et al., Development of ^{225}Ac radiopharmaceuticals: TRIUMF perspectives and experiences. *Curr. Radiopharm.* **11**, 156-172 (2018). <https://doi.org/10.2174/1874471011666180416161908>
- [36] Y.S. Kim, M.W. Brechbiel., An overview of targeted alpha therapy. *Tumor Biol.* **33**, 573-590 (2012). <https://doi.org/10.1007/s13277-011-0286-y>
- [37] A.A.Al. Qaaod, V. Gulik, ^{226}Ra irradiation to produce ^{225}Ac and ^{213}Bi in an accelerator-driven system reactor. *Nucl. Sci. Tech.* **31**, 44 (2020). <https://doi.org/10.1007/s41365-020-00753-2>
- [38] B. Jiang, J.L. Han, J. Ren et al., Measurement of ^{232}Th (n, γ) cross section at the CSNS Back-n facility in the unresolved resonance region from 4 keV to 100 keV. *Chin. Phys. B* **31**, 060101 (2022) . <https://doi.org/10.1088/1674-1056/ac5394>
- [39] J.C. Wang, J. Ren, W. Jiang et al., Determination of the ^{232}Th (n, γ) cross section from 10 to 200 keV at the Back-n facility at CSNS. *Eur. Phys. J. A* **59**, 224 (2023). <https://doi.org/10.1140/epja/s10050-023-01126-0>
- [40] Experimental Nuclear Reaction Data (EXFOR). <https://www-nds.iaea.org/exfor/>
- [41] J.F. Ziegler, M.D. Ziegler, J.P. Biersack, SRIM—The stopping and range of ions in matter (2010). *Nucl. Instrum. Meth. B* **268**, 1818-1823 (2010). <https://doi.org/10.1016/j.nimb.2010.02.091>
- [42] A. Morgenstern, C. Apostolidis, C. Kratochwil et al., An overview of targeted alpha therapy with $^{225}\text{Actinium}$ and $^{213}\text{Bismuth}$. *Curr. Radiopharm.* **11**, 200-208 (2018). <https://doi.org/10.2174/1874471011666180502104524>
- [43] J.G. Jurcic, Targeted alpha-particle immunotherapy with bismuth-213 and actinium-225 for acute myeloid leukemia. *J. Postgrad. Med. Educ. Res.* **47**, 14-17 (2013). <https://doi.org/10.5005/jp-journals-10028-1051>

- [44] G. Henriksen, P. Hoff, J. Alstad et al., ^{223}Ra for endoradiotherapeutic applications prepared from an immobilized $^{227}\text{Ac}/^{227}\text{Th}$ source. *Radiochim. Acta* **89**, 661-666 (2001). <https://doi.org/10.1524/ract.2001.89.10.661>
- [45] Ø.S. Bruland, S. Nilsson, D.R. Fisher et al., High-linear energy transfer irradiation targeted to skeletal metastases by the α -emitter ^{223}Ra : adjuvant or alternative to conventional modalities? *Clin. Cancer Res.* **12**, 6250s-6257s (2006). <https://doi.org/10.1158/1078-0432.CCR-06-0841>
- [46] S. Nilsson, R.H. Larsen, S.D. Fosså et al., First clinical experience with α -emitting radium-223 in the treatment of skeletal metastases. *Clin. Cancer Res.* **11**, 4451-4459 (2005). <https://doi.org/10.1158/1078-0432.CCR-04-2244>
- [47] G. Vaidyanathan, M. Zalutsky, Astatine radiopharmaceuticals: prospects and problems. *Curr. Radiopharm.* **1**, 177-196 (2008). <https://doi.org/10.2174/1874471010801030177>
- [48] J. J. Orozco, T. Bäck, A. Kenoyer et al., Anti-CD45 radioimmunotherapy using ^{211}At with bone marrow transplantation prolongs survival in a disseminated murine leukemia model. *Blood* **121**, 3759-3767 (2013). <https://doi.org/10.1182/blood-2012-11-467035>
- [49] J.R. Crawford, P. Kunz, H. Yang et al., $^{211}\text{Rn}/^{211}\text{At}$ and ^{209}At production with intense mass separated Fr ion beams for preclinical ^{211}At -based α -therapy research. *Appl. Radiat. Isot.* **122**, 222-228 (2017). <https://doi.org/10.1016/j.apradiso.2017.01.035>
- [50] R.A. Aliev, S.V. Ermolaev, A.N. Vasiliev et al., Isolation of medicine-applicable Actinium-225 from thorium targets irradiated by medium-energy protons. *Solvent Extr. Ion Exch.* **32**, 468-477 (2014). <https://doi.org/10.1080/07366299.2014.896582>
- [51] J.Y. Chen, Y.L. Lv, F. Wang et al., Production and isolation of actinium-225 with a 100 MeV proton cyclotron and solid-phase extraction. *Huaxue Tongbao* **84**, 11 (2021). [10.14159/j.cnki.0441-3776.2021.11.011](https://doi.org/10.14159/j.cnki.0441-3776.2021.11.011)
- [52] V. Radchenko, J.W. Engle, J.J. Wilson et al., Application of ion exchange and extraction chromatography to the separation of actinium from proton-irradiated thorium metal for analytical purposes. *J. Chromatogr. A* **1380**, 55-63 (2015). <https://doi.org/10.1016/j.chroma.2014.12.045>